Single-Step Assembly of Cationic Lipid–Polymer Hybrid Nanoparticles for Systemic Delivery of siRNA

Xian-Zhu Yang,[†] Shuang Dou,[†] Yu-Cai Wang,[†] Hong-Yan Long,[†] Meng-Hua Xiong,[†] Cheng-Qiong Mao,[†] Yan-Dan Yao,[‡] and Jun Wang[†,*]

[†]School of Life Sciences and Hefei National Laboratory for Physical Sciences at the Microscale, University of Science and Technology of China, Hefei, Anhui 230027, People's Republic of China and [‡]Sun-Yat-Sen Memorial Hospital, Sun-Yat-Sen University, Guangzhou, Guangdong 510120, People's Republic of China

ABSTRACT

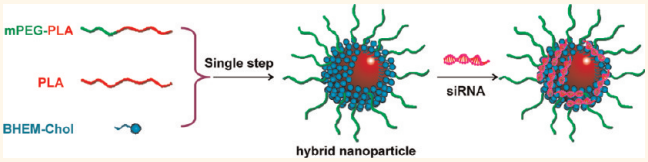

The clinical success of therapeutics of small interfering RNA (siRNA) is still hindered by its delivery systems. Cationic polymer or lipid-based vehicles as the major delivery systems of siRNA cannot sufficiently satisfy siRNA therapeutic applications. It is hypothesized that cationic lipid–polymer hybrid nanoparticles may take advantage of both polymeric and lipid-based nanoparticles for siRNA delivery, while diminishing the shortcomings of both. In this study, cationic lipid–polymer hybrid nanoparticles were prepared by a single-step nanoprecipitation of a cationic lipid (*N*,*N*-bis(2-hydroxyethyl)-*N*-methyl-*N*-(2-cholesteryloxycarbonyl aminoethyl) ammonium bromide, BHEM-Chol) and amphiphilic polymers for systemic delivery of siRNA. The formed hybrid nanoparticles comprised a hydrophobic polylactide core, a hydrophilic poly(ethylene glycol) shell, and a cationic lipid monolayer at the interface of the core and the shell. Such hybrid nanoparticles exhibited excellent stability in serum and showed significantly improved biocompatibility compared to that of pure BHEM-Chol particles. The hybrid nanoparticles were capable of delivering siRNA into BT474 cells and facilitated the escape of loaded siRNA from the endosome into the cytoplasm. The hybrid nanoparticles carrying polo-like kinase 1 (Plk1)-specific siRNA (si*Plk1*) remarkably and specifically downregulated expression of the oncogene Plk1 and induced cancer cell apoptosis both *in vitro* and *in vivo* and significantly suppressed tumor growth following systemic administration. We demonstrate that this system is stable, nontoxic, highly efficient, and easy to scale up, bringing the clinical application of siRNA therapy one important step closer to reality.

KEYWORDS: cationic lipid–polymer hybrid nanoparticles · single-step assembly · siRNA delivery · cancer therapy · polo-like kinase 1

Small interfering RNA (siRNA) has emerged as a potent therapeutic agent for numerous diseases because of its ability to silence specific genes rapidly and efficiently.[1−5] However, the clinical success of RNA interference (RNAi) therapy is still uncertain,[6] and the *in vivo* delivery of siRNA to target sites remains the biggest challenge.[7] Up to now, a variety of systems have been identified and assessed for systemic siRNA delivery and have shown promising efficacy in specific gene silencing and the treatment of various diseases.[8−13] Among these, several are currently undergoing human clinical investigations,[14] including cationic polymer and lipid-based nanoformulations. In general, lipid-based nanoformulations have high efficiency in silencing gene expression and are easy to scale up due to established construction protocols,[15] but their clinical uses are limited due to their instability and toxicity.[16−18] For example, a phase I clinical trial of the first cationic liposome for systemic siRNA delivery sponsored by Tekmira Pharmaceutics (Canada) was terminated due to the potential immune stimulation caused by the liposomes. Cationic polymers, with the proper design, in contrast, have improved stability and biocompatibility over lipids. For instance, no obvious immune response has been observed during the systemic administration of polyplexes from a cyclodextrin-containing polymer and siRNA in a phase I clinical trial.[9,19] However, it still remains challenging to synthesize cationic polymers that can efficiently carry siRNA to cells and silence gene expression because the synthesis of efficient cationic polymer has low reproducibility with high batch-to-batch variation.

It is speculated that cationic lipid–polymer hybrid nanoparticles may take advantage of both polymeric nanoparticles and liposomes in potential clinical applications. Previously, lipid–polymer hybrid nanoparticles were formed by mixing polymeric nanoparticles and lipid-based particles (*e.g.*, liposomes), where the lipid bilayer or lipid multilayer was fused to the surface of polymeric nanoparticles.[20−22] Such preparations usually require a two-step formulation process: (i) the development of

* Address correspondence to jwang699@ustc.edu.cn.

Received for review February 3, 2012 and accepted May 30, 2012.

Published online May 30, 2012
10.1021/nn300500u

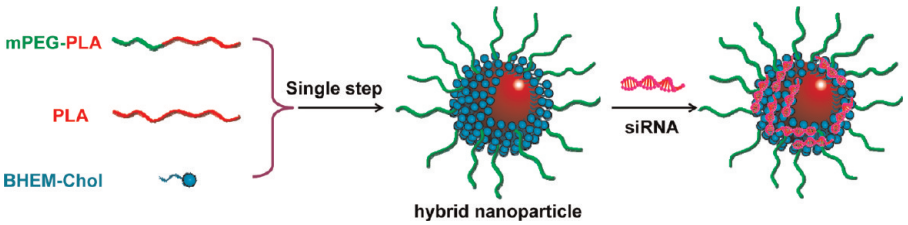

Scheme 1. Schematic illustration of the hybrid nanoparticles prepared through a single-step method and the binding of siRNA. The hybrid nanoparticles comprise a hydrophobic PLA core, a hydrophilic PEG shell, and a cationic lipid (BHEM-Chol) monolayer at the interface of the core and the shell. mPEG-PLA represents poly(ethylene glycol)-*block*-polylactide; PLA represents polylactide, and BHEM-Chol represents *N*,*N*-bis(2-hydroxyethyl)-*N*-methyl-*N*-(2-cholesteryloxycarbonylaminoethyl) ammonium bromide.

polymeric nanoparticles and (ii) their subsequent encapsulation by liposomes, resulting in poor control over the final physicochemical structure of nanoparticles, thus hindering their clinical translation. Zhang *et al.* have recently reported a potent method for the fabrication of lipid−polymer nanoparticles through a single-step nanoprecipitation, which can be used to deliver hydrophobic drugs.[23−25] The hybrid nanoparticles are formed from three components: poly(D,L-lactide-*co*-glycolide) for the hydrophobic core; the neutral lipid DSPE (1,2-distearoyl-*sn*-glycero-3-phosphoethanolamine) for the monolayer surrounding the hydrophobic core; and DSPE-PEG forms the outer shell of the hybrid structure and provides electrostatic and steric stabilization.

In this study, to develop a hybrid nanoparticular system that integrates the desirable characteristics of biodegradable polymer nanoparticles and cationic liposomes for systemic delivery of siRNA, we prepared cationic lipid−polymer hybrid nanoparticles by a single-step nanoprecipitation of a cationic lipid with either amphiphilic poly(ethylene glycol)-*block*-polylactide (mPEG-PLA) or a mixture of mPEG-PLA and polylactide (PLA) (Scheme 1). mPEG-PLA and PLA have already been employed in a variety of clinical applications and have been demonstrated to be safe *in vivo* for several decades.[26,27] The as-formed core−shell hybrid nanoparticles comprised a hydrophobic PLA core, a hydrophilic PEG shell, and a cationic lipid monolayer at the interface of the core and the shell. The hydrophobic PLA core allows the nanoparticle formation first, then siRNA can be efficiently loaded *via* electrostatic interactions with the cationic lipid. The size of the nanoparticles did not show significant change after loading siRNA, which is favorable for the construction of size-controllable siRNA-loaded nanoparticles. This method to form size-controlled siRNA-loaded nanoparticles may display a unique advantage for *in vivo* applications and will be convenient for scaling-up to meet the large quantities required for clinical applications. The formed complex of hybrid nanoparticles and siRNA exhibited excellent serum stability, biocompatibility, efficient carriage of si*Plk1* into cancer cells, and remarkably specific downregulation of Plk1 expression to induce cancer cell apoptosis. The hybrid nanoparticle formulations significantly suppressed tumor growth following systemic administration.

RESULTS AND DISCUSSION

Preparation and Characterization of Hybrid Nanoparticles. In this study, a single-step nanoprecipitation method by addition of amphiphilic polymer solution in acetonitrile to the lipid solution in 10% aqueous ethanol was used to form the hybrid nanoparticles. The hybrid nanoparticles were self-assembled from the mixture of cationic lipid BHEM-Chol, block polymer $mPEG_{5k}$-PLA_{25k}, and homopolymer PLA_{30k} (the subscript number represents the molecular weight, and these molecules are subsequently denoted as mPEG-PLA and PLA, respectively). The mixture of mPEG-PLA and PLA precipitates to form nanoparticles with a core−shell structure, and the cationic lipid self-assembles around the PLA core, as illustrated in Scheme 1.

To investigate the effect of the degree of PEGylation on the structure of formed nanoparticles by this single-step nanoprecipitation method, the nanoparticles were prepared at different PLA/mPEG-PLA weight ratios in the absence of cationic lipid BHEM-Chol. The polymer or polymer mixture in acetonitrile was added dropwise to 10% aqueous ethanol solution under stirring. Nanoparticles from pure PLA easily aggregated and precipitated, while the nanoparticles produced from pure mPEG-PLA or a mixture of mPEG-PLA and PLA polymers (1:1, w/w) were stable with diameters of 100 nm or less, suggesting that PEGylation is required to stabilize such formations. Therefore, PLA/mPEG-PLA with a weight ratio of 1:1 and pure mPEG-PLA were used to fabricate hybrid nanoparticles.

We then produced the hybrid nanoparticles with a similar procedure except that BHEM-Chol was added to the 10% aqueous ethanol solution. The effect of the cationic lipid/polymer weight ratio on the size, polydispersity index (PDI), and zeta-potential of hybrid nanoparticles was investigated. As shown in Figure 1A, nanoparticles from PLA/mPEG-PLA (weight ratio of 1:1) were slightly larger than nanoparticles from mPEG-PLA at a fixed lipid/polymer weight ratio. Incorporating the cationic lipid slightly increased the size of the hybrid nanoparticles. Meanwhile, the PDIs of nanoparticles were not strongly associated with the weight

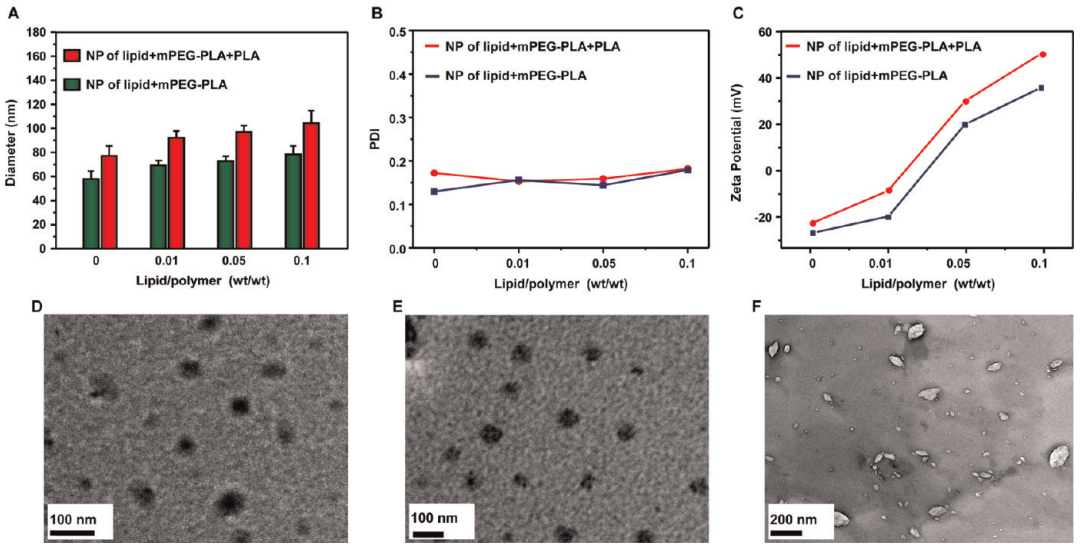

Figure 1. (A−C) Effect of the lipid/polymer weight ratio on size (A), PDI (B), and zeta-potential (C) of formed nanoparticles. NPs of lipid+mPEG-PLA+PLA were prepared using cationic lipid BHEM-Chol and a 1:1 ratio (w/w) of mPEG-PLA and PLA polymers. NPs of lipid+mPEG-PLA were prepared using cationic lipid BHEM-Chol and mPEG-PLA. (D−F) Transmission electronic microscopic images of hybrid $NP_{lipid/mPEG-PLA}$ nanoparticles (D), pure mPEG-PLA nanoparticles (E), and pure BHEM-Chol nanoparticles (F).

ratio of the cationic lipid/polymer (Figure 1B). However, the cationic lipid/polymer weight ratio greatly affected the zeta-potential of the hybrid nanoparticles (Figure 1C); zeta-potential increased as the cationic lipid/polymer weight ratio increased due to the cationic nature of BHEM-Chol. Formulations prepared at higher lipid/polymer weight ratios were also studied. Two populations of particles were detected as the ratio of BHEM-Chol to mPEG-PLA was 2.5:10 (Supporting Information Figure S1). The bigger particles with a diameter of 200 nm were similar to the size of particles prepared with the pure lipid (the typical size was about 60−400 nm). In contrast, particles with a 10% BHEM-Chol/mPEG-PLA weight ratio were similar in size to pure mPEG-PLA nanoparticles. It is believed that, at a 10% BHEM-Chol/mPEG-PLA weight ratio or less, the amount of lipids is in the range to able to cover the surface of the hydrophobic PLA core. However, when the ratio of lipid to polymer was too high, the excess lipids may assemble into liposomes. Therefore, in the following studies, a lipid/polymer weight ratio of 1:10 was used to prepare the hybrid nanoparticles. The hybrid nanoparticles were further denoted as $NP_{lipid/mPEG-PLA}$, where NP represents hybrid nanoparticles and the subscript indicates that the particles were fabricated by BHEM-Chol and mPEG-PLA. Similarly, $NP_{lipid/mPEG-PLA+PLA}$ represents the particles that were fabricated by BHEM-Chol and a mixture of mPEG-PLA and PLA at 1:1 weight ratio.

The morphologies of the obtained nanoparticles were analyzed by transmission electronic microscopy (TEM) (Figure 1D−F). $NP_{lipid/mPEG-PLA}$ exhibited a compact and spherical morphology with a diameter of 65.3 ± 13.5 nm, similar to that of pure mPEG-PLA particles (57.2 ± 12.7 nm). In addition, particles prepared with pure BHEM-Chol were irregular in shape and had a broad size distribution (from 60 to 400 nm). This demonstrates that hybrid nanoparticles were obtained rather than a mixture of distinct liposomes and mPEG-PLA nanoparticles.

Positively charged lipid−polymer hybrid nanoparticles encompass the unique strengths of polymeric nanoparticles and liposomes. The cationic nature of the hybrid nanoparticles allows for the binding of siRNA. As demonstrated by a gel retardation assay, efficient siRNA binding to $NP_{lipid/mPEG-PLA}$ (Figure 2A) and $NP_{lipid/mPEG-PLA+PLA}$ (Figure 2B) occurred at a molar ratio of the BHEM-Chol nitrogen to the siRNA phosphate (N:P) of 5:1. Using a method described in the literature,[28] high-performance liquid chromatography analyses of siRNA concentration in the supernatant after centrifuging the nanoparticles at 300 000*g* for 1 h indicated that the siRNA loading efficiency for $NP_{lipid/mPEG-PLA}$ and $NP_{lipid/mPEG-PLA+PLA}$ was ~95% at the N:P ratio of 5:1 or more.

After siRNA binding, the zeta-potential of $NP_{lipid/mPEG-PLA}$/siRNA and $NP_{lipid/mPEG-PLA+PLA}$/siRNA decreased in water (Figure S2A,B), demonstrating that the positive charge of nanoparticles can be shielded to some extent. Furthermore, the zeta-potentials of $NP_{lipid/mPEG-PLA}$/siRNA and $NP_{lipid/mPEG-PLA+PLA}$/siRNA at the N:P ratio of 10:1 in the Dulbecco's modified Eagle medium (DMEM) were slightly negative (Figure S2C,D). Similar phenomena have been observed by other studies,[29,30] which may be due to the effect of ionic strength.

The cytotoxicities of $NP_{lipid/mPEG-PLA}$, $NP_{lipid/mPEG-PLA+PLA}$, and pure BHEM-Chol nanoparticles were evaluated using the MTT (3-{4,5-dimethylthiazol-2-yl}-2,5-diphenyltetrazolium bromide) assay. As shown in Figure 2C, BHEM-Chol particles exhibited significant

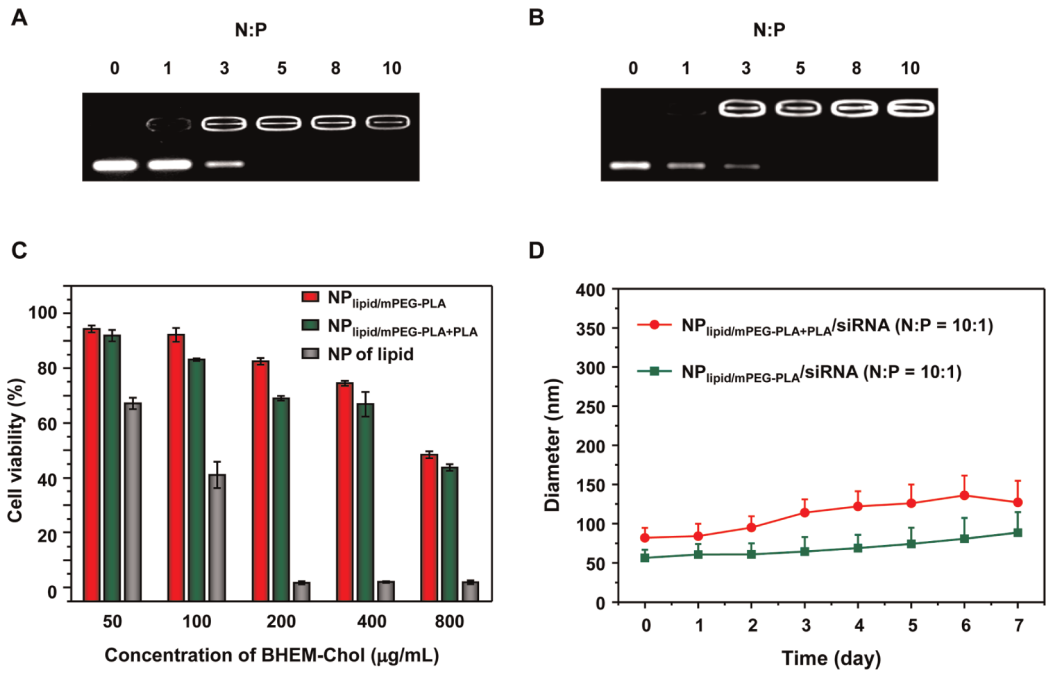

Figure 2. (A,B) Binding ability of hybrid nanoparticles $NP_{lipid/mPEG\text{-}PLA}$ (A) and $NP_{lipid/mPEG\text{-}PLA+PLA}$ (B) to siRNA at different ratios of nitrogen in the carrier to phosphate in the siRNA (N:P ratio) demonstrated by the gel retardation assay. (C) Cytotoxicity of hybrid nanoparticles ($NP_{lipid/mPEG\text{-}PLA}$ and $NP_{lipid/mPEG\text{-}PLA+PLA}$) and particles prepared with only cationic lipid BHEM-Chol (NP of lipid) to BT474 cells by MTT assay. (D) Changes in particle size of the hybrid nanoparticles ($NP_{lipid/mPEG\text{-}PLA}$ and $NP_{lipid/mPEG\text{-}PLA+PLA}$) carrying siRNA at an N:P ratio of 10:1 following incubation with DMEM containing 10% FBS.

cytotoxicity to BT474 cells, particularly at high lipid concentrations. In contrast, even when the total amounts of BHEM-Chol reached up to 0.1 mg mL^{-1} in $NP_{lipid/mPEG\text{-}PLA}$ and $NP_{lipid/mPEG\text{-}PLA+PLA}$, cells treated with these particles showed 90% viability relative to untreated cells. This can be attributed to the masking of cationic charges by the long PEG chains, which can reduce the interaction of BHEM-Chol with cell membranes.

Clinical use of cationic liposomes as systemic delivery vehicles is limited due to their instability, especially when exposed to plasma proteins;[18] we therefore investigated if the hybrid nanoparticles developed in this study can overcome this drawback. Hybrid nanoparticle complexes ($NP_{lipid/mPEG\text{-}PLA}$/siRNA and $NP_{lipid/mPEG\text{-}PLA+PLA}$/siRNA) at a 10:1 N:P ratio were incubated with DMEM containing 10% FBS (fetal bovine serum), and the changes in the size of the complexes at various incubation times were analyzed by dynamic light scattering (DLS) measurements. As shown in Figure 2D, both hybrid nanoparticle types exhibited excellent colloidal stability in medium as demonstrated by consistent diameters after incubation for 7 days. We speculate that the PEG present on the surface of hybrid nanoparticles prevented nonspecific protein adsorption and aggregation of the nanoparticles.

Cellular Internalization and Endosomal Escape of Hybrid Nanoparticles Carrying siRNA. BT474 cells were incubated with either $NP_{lipid/mPEG\text{-}PLA}$/siRNA or $NP_{lipid/mPEG\text{-}PLA+PLA}$/siRNA complexes at an N:P ratio of 10:1 to evaluate their cellular uptake. Fluorescent FAM-labeled siRNA was used to track the nanoparticles. As shown in Figure 3, FAM-siRNA was observed within the BT474 cells after 1 h of incubation, indicating the internalization of $NP_{lipid/mPEG\text{-}PLA}$ and $NP_{lipid/mPEG\text{-}PLA+PLA}$.

To more precisely understand how the composition of formulations affected cell internalization of siRNA, we incubated $NP_{lipid/mPEG\text{-}PLA}$/FAM-siRNA or $NP_{lipid/mPEG\text{-}PLA+PLA}$/FAM-siRNA with BT474 cells for 1 h and subsequently analyzed the cells by flow cytometry after quenching the extracellular fluorescence with trypan blue. As shown in Figure 3B,C, cells incubated with $NP_{lipid/mPEG\text{-}PLA+PLA}$/FAM-siRNA complexes exhibited stronger intracellular fluorescence than those incubated with $NP_{lipid/mPEG\text{-}PLA}$/FAM-siRNA complexes at N:P ratios of 5:1 and 10:1. This occurred because $NP_{lipid/mPEG\text{-}PLA}$ has a higher degree of PEGylation than $NP_{lipid/mPEG\text{-}PLA+PLA}$, which inhibits cellular uptake. In addition, it should be noted that, for both complexes, the fluorescence intensities of BT474 cells incubated with both FAM-siRNA-loaded hybrid nanoparticles were improved with an increase in the N:P ratio.

Lysosomal escape of siRNA after entering the cell is important for subsequent post-transcriptional gene silencing in the cytoplasm.[7] To investigate whether siRNA loaded into the hybrid nanoparticles could escape from the endosome/lysosome, BT474 cells were treated with $NP_{lipid/mPEG\text{-}PLA+PLA}$/FAM-siRNA at N:P ratio of 10:1 for different periods of time, and the localization of nanoparticles in cells was observed by

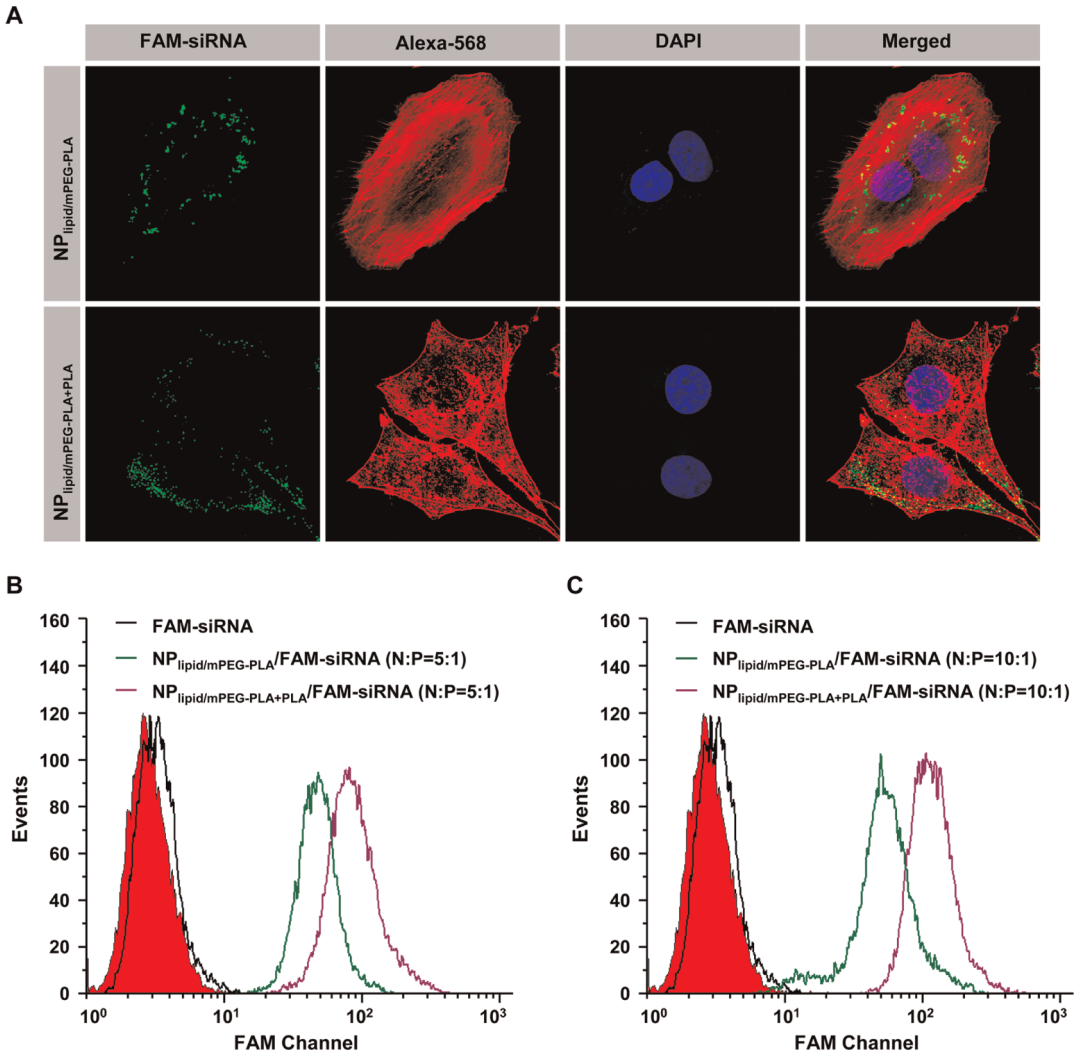

Figure 3. (A) CLSM (confocal laser scanning microscope) images of cell internalization of $NP_{lipid/mPEG\text{-}PLA}$/FAM-siRNA and $NP_{lipid/mPEG\text{-}PLA+PLA}$/FAM-siRNA complexes (N:P = 10:1) in BT474 cells after 1 h of incubation. Cell cytoskeleton F-actin and cell nuclei were counterstained with Alexa Fluor 568 phalloidin and DAPI, respectively. (B,C) Flow cytometric analyses of BT474 cells after 1 h of incubation with $NP_{lipid/mPEG\text{-}PLA}$/FAM-siRNA and $NP_{lipid/mPEG\text{-}PLA+PLA}$/FAM-siRNA complexes at N:P ratios of 5:1 (B) and 10:1 (C), respectively. The negative control was incubated with PBS. The final concentration of FAM-siRNA in the culture medium was 200 nM.

staining the acidic organelles (including endosomes and early lysosomes) with LysoTracker Red. The cell nuclei were counterstained with DAPI. As shown in Figure 4, both $NP_{lipid/mPEG\text{-}PLA+PLA}$ and $NP_{lipid/mPEG\text{-}PLA}$ carrying FAM-siRNA (green) were mainly colocalized with the LysoTracker Red stained organelles after 2 h of incubation, indicating that these hybrid nanoparticles resided in endosomes or early lysosomes. However, after 4 and 8 h of incubation, the separation of the green and red fluorescence was more significant when the cells were incubated with $NP_{lipid/mPEG\text{-}PLA+PLA}$/FAM-siRNA, suggesting that FAM-siRNA more efficiently escaped from the lysosomal vesicles following the delivery of $NP_{lipid/mPEG\text{-}PLA+PLA}$; this is likely due to the fact that PEGylation inhibits the endosomal/lysosomal escape of nanoparticles.[31]

Downregulation of Gene Expression and Induction of Cell Apoptosis *in Vitro*. Before the gene silencing application, the cytotoxicities of $NP_{lipid/mPEG\text{-}PLA+PLA}$/siRNA and $NP_{lipid/mPEG\text{-}PLA}$/siRNA were evaluated in B7474 cells using the MTT assay. As shown in Figure S3, both $NP_{lipid/mPEG\text{-}PLA+PLA}$/siRNA and $NP_{lipid/mPEG\text{-}PLA}$/siRNA at N:P ratios of 5:1 and 10:1 showed nearly 100% viability relative to untreated cells at a si*N.C.* dose of 200 nM. Next, we evaluated the downregulation of the therapeutic target gene by siRNA-loaded nanoparticles. The Plk1 gene was selected since it is a well-known key regulator of mitotic progression in mammalian cells that shows elevated activity in many cancers.[32,33] BT474 cells were incubated with hybrid nanoparticles carrying si*Plk1* (200 nM) at N:P ratios of 5:1 and 10:1, and gene expression was analyzed after 24 h by quantitative real-time polymerase chain reaction (qRT-PCR). As shown in Figure 5A, the negative control siRNA (si*N.C.*)-loaded nanoparticles did not downregulate Plk1 expression. In contrast, both

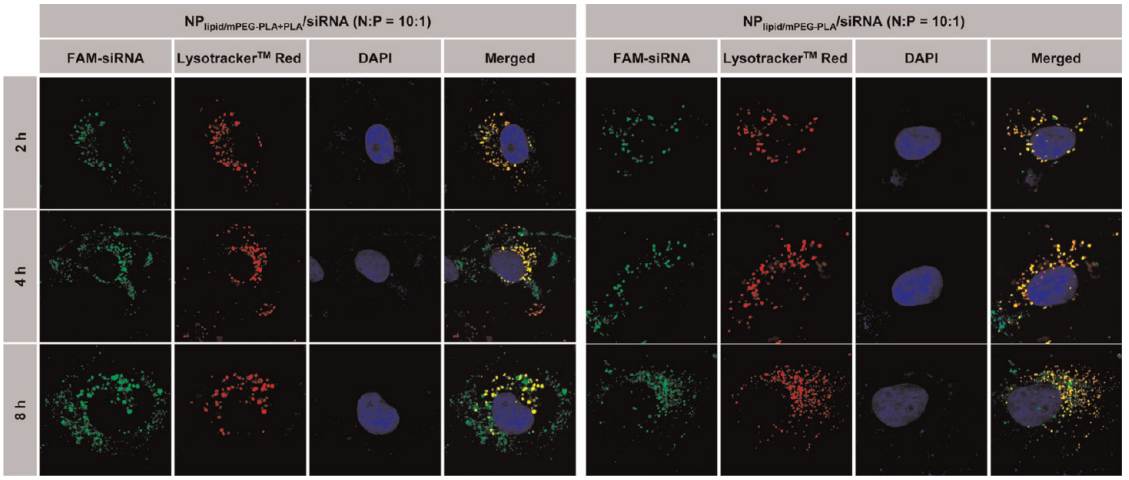

Figure 4. Assessment by CLSM of endosomal escape of $NP_{lipid/mPEG\text{-}PLA+PLA}$/FAM-siRNA and $NP_{lipid/mPEG\text{-}PLA}$/FAM-siRNA at an N:P ratio of 10:1 in BT474 cells after incubation with cells for different times. The final concentration of FAM-siRNA in the culture medium was 200 nM. Cell nuclei and endosomes/lysosomes were counterstained with DAPI (blue) and LysoTracker Red (red).

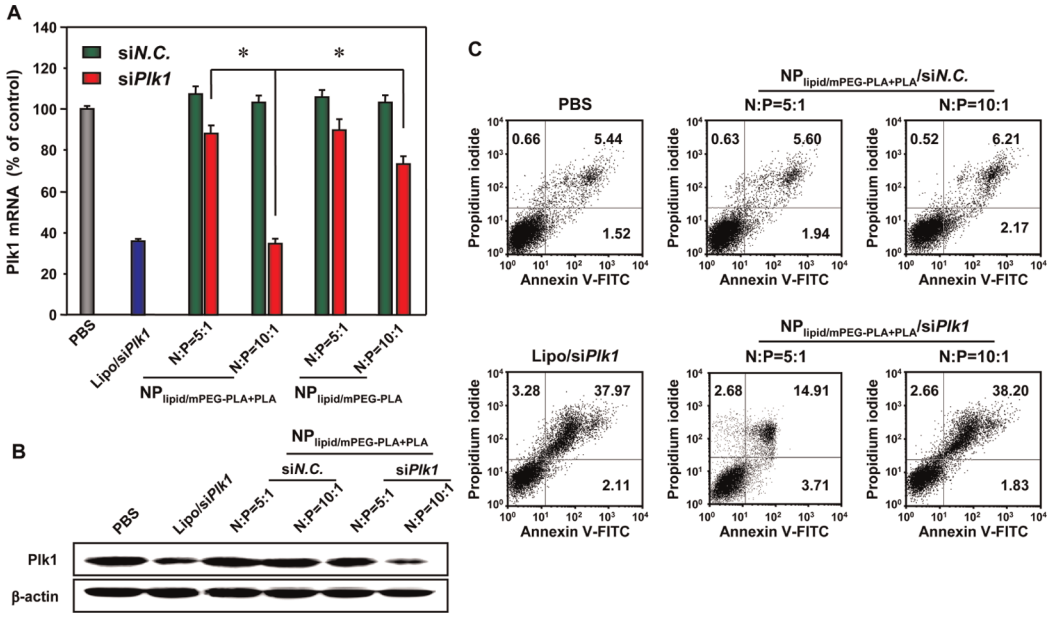

Figure 5. (A) Plk1 mRNA expression determined by quantitative real-time PCR. (B) Plk1 protein expression determined by Western blot analysis. (C) Cell apoptosis following transfection with different formulations. Early apoptotic cells are shown in the lower right quadrant, and late apoptotic cells are shown in the upper right quadrant. $NP_{lipid/mPEG\text{-}PLA+PLA}$/si*N.C.* (or $NP_{lipid/mPEG\text{-}PLA}$/si*N.C.*) and $NP_{lipid/mPEG\text{-}PLA+PLA}$/si*Plk1* (or $NP_{lipid/mPEG\text{-}PLA}$/si*Plk1*) represent cells that were transfected with hybrid nanoparticles $NP_{lipid/mPEG\text{-}PLA+PLA}$ (or $NP_{lipid/mPEG\text{-}PLA}$) carrying si*N.C.* (200 nM) and si*Plk1* (200 nM), respectively. Lipo/si*Plk1* represents cells that were transfected with complexes of Lipofectamine 2000 with si*Plk1* (50 nM).

$NP_{lipid/mPEG\text{-}PLA+PLA}$/si*Plk1* and $NP_{lipid/mPEG\text{-}PLA}$/si*Plk1* downregulated Plk1 gene expression in cells after culturing with the nanoparticles. Notably, $NP_{lipid/mPEG\text{-}PLA+PLA}$/si*Plk1* was more effective than $NP_{lipid/mPEG\text{-}PLA}$/si*Plk1* in the case of gene silencing at both N:P ratios, due to the greater amount of siRNA internalization by the cells and more efficient escape of siRNA from the endosome and lysosome, as demonstrated in Figure 3B,C and Figure 4. Moreover, we observed that the gene silencing efficiency of both hybrid nanoparticles was N:P ratio-dependent; increasing the N:P ratio from 5:1 to 10:1 enhanced the inhibition of gene expression. For example, $NP_{lipid/mPEG\text{-}PLA+PLA}$/si*Plk1* at the 10:1 N:P ratio significantly decreased Plk1 expression (35.3% of the PBS control, $p < 0.01$) in cells compared to that at an N:P ratio of 5:1 (71.0% of the PBS control), reaching a similar level to that of Lipofectamine 2000 (36.6% of the PBS control). This phenomenon was consistent with the improved siRNA internalization as a result of the increased N:P ratio (Figure 3B,C).

The reduction in Plk1 mRNA decreased Plk1 protein expression in the cells. Western blot analyses were used to detect Plk1 protein expression levels after the

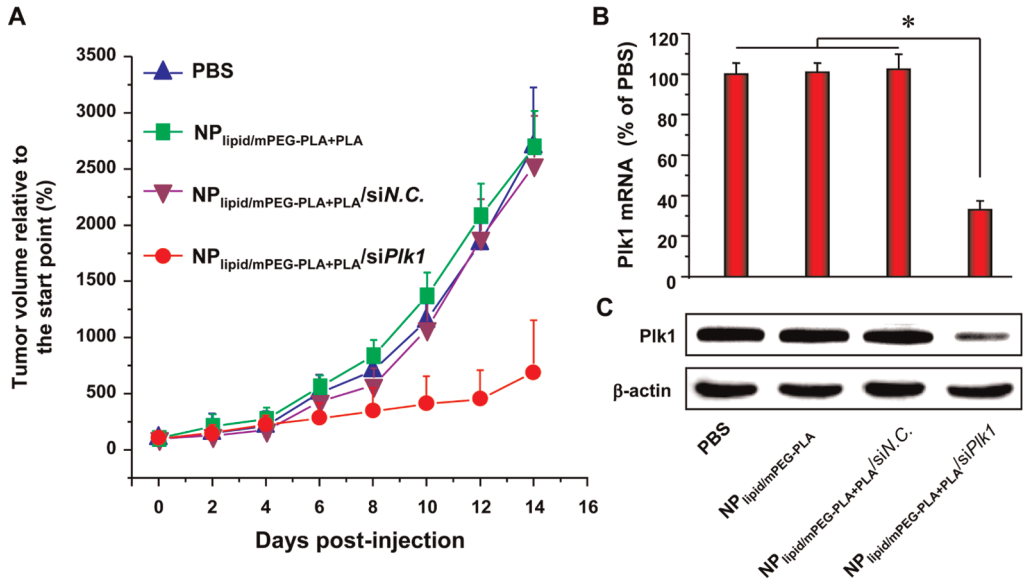

Figure 6. (A) Inhibition of tumor growth in a murine model with BT474 xenografts after treatment with various formulations ($n = 6$). (B,C) Expression of Plk1 mRNA (B) and protein (C) in tumors was analyzed 24 h after the final injection. BT474 xenograft tumor-bearing mice received one intravenous injection everyday from the 10th day post-xenograft implantation in all of the experiments. $NP_{lipid/mPEG-PLA+PLA}$, $NP_{lipid/mPEG-PLA+PLA}$/si*N.C.*, and $NP_{lipid/mPEG-PLA+PLA}$/si*Plk1* represent that the mice were administered with empty hybrid nanoparticles $NP_{lipid/mPEG-PLA+PLA}$, $NP_{lipid/mPEG-PLA+PLA}$ carrying si*N.C.*, and si*Plk1* at the same weight of hybrid nanoparticles (3.05 mg per injection), respectively. The N:P ratios were all 10:1 in the experiments, and the dose of siRNA was 10 μg per mouse per injection; * $p < 0.005$ ($n = 6$). Days after the first injection.

cells were incubated for 48 h with $NP_{lipid/mPEG-PLA+PLA}$/si*Plk1* at N:P ratios of 5:1 and 10:1. As shown in Figure 5B, delivery of si*Plk1* by $NP_{lipid/mPEG-PLA+PLA}$ decreased Plk1 protein expression at both N:P ratios. Furthermore, si*Plk1*-loaded $NP_{lipid/mPEG-PLA+PLA}$ exhibited significantly improved silencing of Plk1 protein expression at the N:P ratio of 10:1 compared to at the N:P ratio of 5:1. In addition, si*N.C.*-loaded $NP_{lipid/mPEG-PLA+PLA}$ at N:P ratios of 5:1 and 10:1 did not downregulate Plk1 protein expression in BT474 cells, indicating that no nonspecific gene silencing occurred.

It has been reported that Plk1 inhibition increases cancer cell apoptosis.[34] Apoptosis in BT474 cells was evaluated after transfection with various nanoparticle and siRNA loading formulations by staining with Annexin V-FITC and propidium iodide (PI) (Figure 5C). Incubation with $NP_{lipid/mPEG-PLA+PLA}$/si*Plk1* (200 nM) at an N:P ratio of 10:1 induced apoptosis in 39.94% of BT474 cells, while incubation with $NP_{lipid/mPEG-PLA+PLA}$/si*Plk1* at an N:P ratio of 5:1 (same total si*Plk1* dosage) induced apoptosis in only 18.62% of BT474 cells. Moreover, $NP_{lipid/mPEG-PLA+PLA}$/si*N.C.* (at the same siRNA dose as with si*Plk1*) did not induce apoptosis, demonstrating that apoptosis was due to Plk1 downregulation.

***In Vivo* Tumor Growth Suppression.** To reveal the potential of such hybrid nanoparticles as an siRNA delivery system *in vivo*, fluorescent coumarin-6 was incorporated into the nanoparticles, and the blood concentrations of coumarin-6 were determined with an HPLC fluorescence detection method. As shown in Figure S4A, $NP_{lipid/mPEG-PLA+PLA}$/si*Plk1* and nanoparticles of mPEG-PLA and PLA ($NP_{mPEG-PLA+PLA}$) exhibited similar concentration−time profiles, and the half-life of $NP_{lipid/mPEG-PLA+PLA}$/si*Plk1* and $NP_{mPEG-PLA+PLA}$ was 222.2 and 308.1 min, respectively. Furthermore, the biodistribution of $NP_{lipid/mPEG-PLA+PLA}$/si*Plk1* and $NP_{mPEG-PLA+PLA}$ was examined 24 h after the intravenous injection in a mouse bearing the BT474 xenograft. The strongest fluorescence was detected at the tumor site (Figure S4B), demonstrating the accumulation of $NP_{lipid/mPEG-PLA+PLA}$/si*Plk1* in tumor tissue. It is speculated that the PEG shell prevented nonspecific protein adsorption and aggregation of the nanoparticles *in vivo*, thus $NP_{lipid/mPEG-PLA+PLA}$/si*Plk1* accumulated at the tumor site through the "enhanced permeation and retention" (EPR) effect.[35]

Next, we examined the antitumor growth effect of $NP_{lipid/mPEG-PLA+PLA}$/si*Plk1* after accumulation in the tumor site. Athymic mice bearing BT474 xenografts each received a daily intravenous injection of $NP_{lipid/mPEG-PLA+PLA}$/si*Plk1* at an siRNA dose of 10 μg per injection. Unloaded $NP_{lipid/mPEG-PLA+PLA}$ and $NP_{lipid/mPEG-PLA+PLA}$/si*N.C.* at the same polymer weights were used as negative controls. As shown in Figure 6A, intravenous injection of $NP_{lipid/mPEG-PLA+PLA}$/si*Plk1* inhibited tumor growth, whereas neither $NP_{lipid/mPEG-PLA+PLA}$/si*N.C.* nor unloaded $NP_{lipid/mPEG-PLA+PLA}$ slowed tumor growth. This shows that si*Plk1*, the delivery of which was mediated by $NP_{lipid/mPEG-PLA+PLA}$, was responsible for tumor suppression.

To demonstrate that retarded tumor growth by $NP_{lipid/mPEG-PLA+PLA}$/si*Plk1* was related to Plk1 downregulation in tumor cells, the tumors were excised 24 h

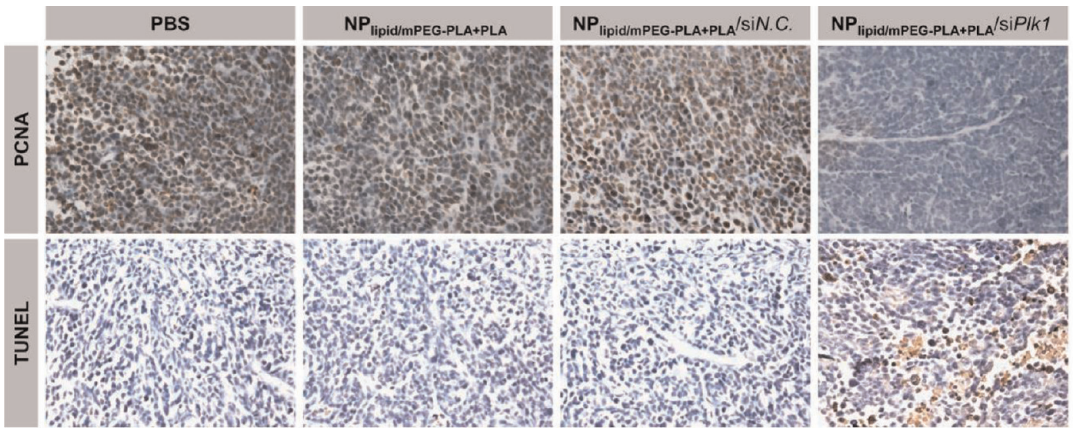

Figure 7. PCNA and TUNEL analyses of tumor tissues after treatment with various formulations. The tumor tissues were collected 24 h after the last injection. $NP_{lipid/mPEG\text{-}PLA+PLA}$, $NP_{lipid/mPEG\text{-}PLA+PLA}$/si*N.C.*, and $NP_{lipid/mPEG\text{-}PLA+PLA}$/si*Plk1* represent that the mice were administered with empty hybrid nanoparticles $NP_{lipid/mPEG\text{-}PLA+PLA}$, $NP_{lipid/mPEG\text{-}PLA+PLA}$ carrying si*N.C.*, and si*Plk1* at the same weight of hybrid nanoparticles (3.05 mg per injection), respectively. The N:P ratios were 10:1 in all of the experiments, and the dose of siRNA was 10 μg per mouse per injection.

after the last injection. Tumoral Plk1 mRNA and protein expression were analyzed by qRT-PCR and Western blot analyses, respectively. Plk1 mRNA levels showed a 65% reduction after treatment with $NP_{lipid/mPEG\text{-}PLA+PLA}$/si*Plk1* when compared to the level in tumors following treatments with PBS ($p < 0.005$, Figure 6B). Treatments with the negative controls did not show reductions in Plk1 mRNA levels in the tumor when compared to the PBS control. Western blot analyses of Plk1 protein levels in each tumor mass (Figure 6C) revealed a significant reduction in Plk1 protein levels when the mice were treated with $NP_{lipid/mPEG\text{-}PLA+PLA}$/si*Plk1*. In contrast, there was no significant decrease in Plk1 protein levels after treatments with either unloaded $NP_{lipid/mPEG\text{-}PLA+PLA}$ or $NP_{lipid/mPEG\text{-}PLA+PLA}$/si*N.C.* when compared with the treatment with the PBS control. These results demonstrate that tumor growth suppression was due to downregulation of the Plk1 gene after treatment with $NP_{lipid/mPEG\text{-}PLA+PLA}$/si*Plk1*.

Cell proliferation and apoptosis in the tumors after treatment with various formulations were analyzed by immunohistochemical staining of proliferating cell nuclear antigen (PCNA) and the terminal deoxynucleotidyl transferase-mediated dUTP nick end-labeling (TUNEL) assay, respectively. As shown in Figure 7, treatment with $NP_{lipid/mPEG\text{-}PLA+PLA}$/si*Plk1* resulted in a remarkable decrease in PCNA-positive tumor cells (brown), indicating the inhibition of cell proliferation in breast tumor tissue. The administration of si*Plk1*-loaded nanoparticles also increased cell apoptosis, as shown by TUNEL-positive tumor cells (brown). In contrast, blank $NP_{lipid/mPEG\text{-}PLA+PLA}$ and $NP_{lipid/mPEG\text{-}PLA+PLA}$/si*N.C.* did not significantly inhibit cell proliferation as demonstrated by the insignificant change in the number of proliferating PCNA-positive tumor cells and TUNEL-positive tumor cells when compared with the PBS treatments.

CONCLUSION

We have developed cationic lipid−polymer hybrid nanoparticles that can be created by single-step nanoprecipitation, which can efficiently load siRNA. The composition of formulation affected cellular uptake of the nanoparticles and gene silencing efficacy both *in vitro* and *in vivo*. The hybrid nanoparticles were highly stable, capable of delivering siRNA into BT474 cells, and facilitated the escape of loaded siRNA from the endosome into the cytoplasm, causing remarkable and specific downregulation of targeted Plk1 oncogene and consequent cancer cell apoptosis. Moreover, the hybrid nanoparticles, by delivering si*Plk1*, were able to inhibit tumor growth in a BT474 xenograft murine model by silencing the Plk1 gene in tumor cells. All of these findings show that this hybrid nanoparticle formulation has remarkable potential as an siRNA delivery carrier for cancer therapy.

MATERIALS AND METHODS

Materials and Characterization. Dulbecco's modified Eagle medium (DMEM) and MTT were purchased from Gibco BRL (Eggenstein, Germany). The Lipofectamine 2000 transfection kit from Invitrogen (Carlsbad, USA) was used as suggested by the supplier. Fluorescently labeled FAM-siRNA and negative control siRNA with a scrambled sequence (si*N.C.*, antisense strand, 5′-AACCACTCAACTTTTTCCCAAdTdT-3′) and siRNA targeting Plk1 mRNA (si*Plk1*, antisense strand, 5′-UAAGGAGGGUGAUCUUCUUCAdTdT-3′) were synthesized by Suzhou Ribo Life Science Co. (Kunshan, China). Other organic solvents or reagents were analytical grade and used as received.

BHEM-Chol and block polymer $mPEG_{5k}$-PLA_{25k} were synthesized according to our previously reported procedure.[28] Homopolymer PLA_{30k} was synthesized using a procedure reported in

the literature,[36] and the molecular weights were determined by ^{1}H NMR (data not shown).

Preparation of Hybrid Nanoparticles. Cationic lipid−polymer hybrid nanoparticles were prepared by a modified nanoprecipitation method. Briefly, $mPEG_{5k}$-PLA_{25k} or its mixture with PLA_{30k} (10 mg) was dissolved in acetonitrile at a concentration of 2 mg/mL. The cationic lipid BHEM-Chol was dissolved in 10% aqueous ethanol solution, which was preheated at 70 °C for 10 min. The polymer solution was added dropwise to the lipid solution under vigorous stirring. Afterward, the mixed solution was gently stirred for 2 h at room temperature. The nanoparticles were washed three times with ultrapurified water and collected by centrifugation at 300 rpm (Sorvall, Biofuge Stratos, Germany) with an Amicon Ultra-4 centrifuge filter (molecular weight cutoff of 10 kDa, Millipore, Billerica, MA).

Characterization of Cationic Lipid−Polymer Hybrid Nanoparticles. The diameters, PDIs, and zeta-potential of the nanoparticles in water were analyzed by a Malvern Zetasizer Nano ZS90 apparatus at 25 °C, illuminating the sample with 633 nm wavelength radiation from a solid-state He−Ne laser and collecting the scattered light at an angle of 90°. The nanoparticles were analyzed in triplicate at a concentration of 1.0 mg/mL. The intensity-average hydrodynamic particle size and PDI were obtained with Malvern's Zetasizer Nano 4.2 software.[37] Zeta-potential measurements were obtained in a disposable capillary (DTS1060). The Smoluchowski approximation was used to convert mobilities into zeta-potentials.[38]

The morphology of the hybrid nanoparticles was examined by JEOL-2010 transmission electron microscopy (TEM) at an accelerating voltage of 200 kV.

Preparation of Hybrid Nanoparticles/siRNA Complexes and Gel Retardation Assay. For siRNA loading, the nanoparticles were diluted to different concentrations for desired N:P ratios using either water or medium and added to siRNA solution (20 mM). The N:P ratio was defined as the residual molar ratio of amine units in the cationic lipid to phosphate units in the siRNA. The mixture was mixed by pipetting and allowed to stand for 20 min before use.

Various complexes were prepared at different N:P ratios ranging from 1:1 to 10:1 as described above. The complexes were electrophoresed on a 1.5% agarose gel at a constant voltage of 120 V for 5 min in Tris/borate/EDTA buffer (TBE buffer; 89 mM Tris, 89 mM boric acid, 2 mM EDTA, pH 8.3). The siRNA bands were visualized with ethidium bromide staining under a UV transilluminator at a wavelength of 365 nm. Free siRNA was used as the control.

Colloidal Stability of Hybrid Nanoparticles Carrying siRNA. The cationic hybrid nanoparticle/siRNA complexes at a concentration of 1 mg/mL were incubated in DMEM containing 10% FBS (Hyclone, Waltham, MA) at 37 °C under gentle stirring. At each time point, the mean diameters of nanoparticles were monitored as described above using a Malvern Zetasizer Nano ZS90 apparatus as described above.

Cell Culture. The human breast cancer cell BT474 from the American Type Culture Collection (ATCC) was maintained in DMEM supplemented with 10% FBS and 4 mM L-glutamine (Sigma-Aldrich, St. Louis, MO). Cells were incubated at 37 °C in a 5% CO_2 atmosphere.

Cytotoxicity Measurement. The cytotoxicity of the nanoparticles was assessed by an MTT viability assay against BT474 cells. Cells were seeded in 96-well plates at 10 000 cells per well in 100 μL of complete DMEM supplemented with 10% FBS and incubated at 37 °C in a 5% CO_2 atmosphere for 24 h. To determine the cytotoxicity of nanoparticles, 100 μL of various nanoparticles in complete DMEM at different concentrations was used to replace the culture medium, and cells were further cultured for 24 h. MTT stock solution was then added to each well to achieve a final concentration of 1 g/L, with the exception of the wells used as a blank, to which the same volume of phosphate buffered saline (PBS, 0.01 M, pH 7.4) was added. After incubation for an additional 2 h, 125 μL of the extraction buffer (20% SDS in 50% DMF, pH 4.7, prepared at 37 °C) was added to the wells and incubated overnight at 37 °C. The absorbance was measured at 570 nm using a Bio-Rad 680 microplate reader. Cell viability was normalized to that of BT474 cells cultured in the culture medium with PBS treatment.

The cytotoxicities of $NP_{lipid/mPEG\text{-}PLA+PLA}$/siRNA and $NP_{lipid/mPEG\text{-}PLA}$/siRNA to BT474 cells were also evaluated using the MTT assay. BT474 cells were seeded in 96-well plates at 10 000 cells per well. After 24 h of incubation, 100 μL of $NP_{lipid/mPEG\text{-}PLA+PLA}$/siRNA and $NP_{lipid/mPEG\text{-}PLA}$/siRNA in complete DMEM at N:P ratios of 5:1 and 10:1 was used to replace the culture medium. si*N.C.* was used in the assay, and the final concentration of si*N.C.* in the culture medium was 200 nM. After 48 h of incubation, an MTT assay was performed as described above to determine the percentage of viable cells remaining after treatment with different complexes.

Cellular Uptake of Hybrid Nanoparticles and Intracellular Trafficking. For microscopic observation, BT474 cells (5×10^4 cells/well) were seeded on coverslips in a 24-well plate and incubated for 24 h. Hybrid nanoparticles carrying FAM-siRNA were added and incubated with the cells. The final concentration of FAM-siRNA in the culture medium was 200 nM. After 1 h of incubation, cells were washed twice with PBS and fixed with 4% formaldehyde for 15 min at room temperature. The cells were stained with Alexa Fluor 568 phalloidin (Invitrogen, Carlsbad, CA) to indicate the cytoskeleton and counterstained with DAPI to indicate cell nuclei according to the standard protocol provided by the suppliers. Coverslips were mounted on glass microscope slides with a drop of antifade mounting media (Sigma-Aldrich) to reduce fluorescent photobleaching. The cellular uptake of nanoparticles was visualized by CLSM (LSM 710, Carl Zeiss Inc., Jena, Germany).

For flow cytometric analysis, BT474 cells were seeded into 24-well plates at 5×10^4 cells per well in 0.5 mL of complete DMEM and cultured at 37 °C in a 5% CO_2 humidified atmosphere for 24 h. The original medium was replaced with FAM-siRNA-formulated hybrid nanoparticles. The FAM-siRNA concentration was 200 nM. The cells were incubated 1 h at 37 °C and were then rinsed twice with cold PBS. The cells were trypsinized, washed with cold PBS, and treated for 5 min with trypan blue (0.2 mg/mL in PBS) to quench the extracellular fluorescence. The cells were further washed with cold PBS, filtered through 35 μm nylon mesh, and subjected to flow cytometric analysis using a BD FACSCalibur flow cytometer.

To follow the endosomal release of nanoparticles, after different incubation times with hybrid nanoparticles containing FAM-siRNA (200 nM siRNA), BT474 cells were washed with PBS and stained with LysoTracker Red (Molecular Probe, Eugene, OR) following the manufacturer's instructions. The cells were then washed twice with PBS, fixed with 4% formaldehyde for 15 min, and counterstained with DAPI. The cells were imaged by CLSM to determine the localization of siRNA inside the cells.

***In Vitro* Gene Silencing.** To assess the silencing capability of hybrid nanoparticles, BT474 cells were seeded into 6-well plates (2×10^5 per well) and incubated for 24 h. The cells were transfected with various formulations at a final siRNA dose of 200 nM. Lipofectamine 2000 carrying 50 nM of si*Plk1* was used as the positive control. After further incubation for 24 h (for mRNA isolation) or 48 h (for protein extraction) at 37 °C, the cellular levels of Plk1 mRNA and protein were assessed using qRT-PCR and Western blot, respectively.

For qRT-PCR analysis, the cells were collected and total RNA from transfected cells was isolated using an RNeasy mini kit (Qiagen, Valencia, CA) according to the manufacturer's protocol. Two micrograms of total RNA was transcribed into cDNA using the PrimeScript First Strand cDNA Synthesis Kit (Takara, Dalian, China). Thereafter, 2 μL of cDNA was subjected to qRT-PCR analysis targeting Plk1 and glyceraldehyde 3-phosphate dehydrogenase (GAPDH) using the SYBR Premix Ex Taq (Perfect Real Time) (Takara, Dalian, China). Analysis was performed using the Applied Biosystems StepOne Real-Time PCR Systems. Relative gene expression values were determined by the $\Delta\Delta CT$ method using StepOne software v2.1 (Applied Biosystems). Data are presented as the fold difference in Plk1 expression normalized to the housekeeping gene GAPDH as the endogenous reference and relative to the untreated control cells. The primers used in the quantitative real-time PCR for Plk1 and GAPDH were 5′-AGCCTGAGGCCCGATACTACCTAC-3′ (Plk1-forward), 5′-ATTAGGAGTCCCACACAGGGTCTTC-3′ (Plk1-reverse), and 5′-TTCACCACCATGGAGAAGGC-3′ (GAPDH-forward),

5′-GGCATGGACTGTGGTCATGA-3′ (GAPDH-reverse). PCR parameters consisted of 30 s of Taq activation at 95 °C, followed by 40 cycles of PCR at 95 °C × 5 s, 60 °C × 30 s, and 1 cycle of 95 °C × 15 s, 60 °C × 60 s, and 95 °C × 15 s. Standard curves were generated, and the relative amount of target gene mRNA was normalized to GAPDH mRNA. Specificity was verified by melt curve analysis.

In Western blot analysis, transfected cells were first washed twice with cold PBS, then resuspended in 50 μL of lysis buffer (50 mM HEPES, pH 7.5, 150 mM NaCl, 1% Triton X-100, 10% glycerol, 1.5 mM $MgCl_2$, 1 mM EGTA) freshly supplemented with Roche's Complete Protease Inhibitor Cocktail Tablets. The cell lysates were incubated on ice for 1 h and vortexed every 5 min. The lysates were then clarified by centrifugation for 10 min at 12 000*g*. The protein concentration was determined using the BCA Protein Assay Kit (lot: 23250, Thermo, Madison, WI). Total protein (100 μg) was separated on 12% bis-Tris-polyacrylamide gels and then transferred (at 300 mA for 45 min) to Immobilon-P membranes (Millipore, Bedford, MA). After incubation in 5% bovine serum albumin (BSA, Sigma-Aldrich) in phosphate buffered saline with Tween-20 (PBST, pH 7.2) for 2 h, the membranes were incubated in 1% BSA in PBS with monoclonal antibodies against Plk1 (1:1000) overnight. The membrane was incubated in 1% BSA with goat anti-mouse IgG-HRP antibody (1:10 000) for 30 min, and bands were visualized using ImageQuant LAS 4000 mini (GE Healthcare).

Cell Apoptosis Analysis. BT474 cells were seeded into 24-well plates (1.0×10^5 per well) and incubated for 24 h. The cells were treated with the above-mentioned formulations. Lipofectamine 2000 carrying si*Plk1* (50 nM) was used as the positive control. After 48 h of incubation, the cells were collected and the apoptotic cells were detected by flow cytometry using the annexin V-FITC apoptosis detection kit I (BD Biosciences, San Diego, CA) according to the standard protocol provided by the suppliers. The results were analyzed using WinMDI 2.9 software.

Human Breast Cancer Xenograft Tumor Model and Tumor Suppression Study. BALB/cA-nu nude mice (6 weeks old) were purchased from the Beijing HFK Bioscience Co., LTD (Beijing, China), and all animals received care in compliance with the guidelines outlined in the *Guide for the Care and Use of Laboratory Animals*. The procedures were approved by the University of Science and Technology of China Animal Care and Use Committee.

The xenograft tumor model was generated by subcutaneous injection of BT474 cells (1×10^7 for each mouse) in the mammary fat pad of the mouse. When the tumor volume was around 50 mm^3 at 10 days after cell implantation, the mice were randomly divided into four groups (six mice per group) and treated with PBS, blank hybrid nanoparticles, hybrid nanoparticles carrying si*Plk1*, or control si*N.C.* by intravenous injection. The mouse received daily injections at a dose of 10 μg siRNA per mouse. Tumor growth was monitored by measuring the perpendicular diameter of the tumor using calipers. The estimated volume was calculated according to the following formula: tumor volume (mm^3) = 0.5 × length × $width^2$.

Detection of Plk1 Expression in Tumor Tissues. Tumor tissues were collected 24 h after the last intravenous injection. Plk1 expression at mRNA and protein levels in the tumors was analyzed by qRT-PCR and Western blot analyses.

For Plk1 mRNA analysis, a piece of tumor tissue (~10 mg) was lysed using the RNeasy mini kit. The mRNA was collected and analyzed by qRT-PCR as described above.

For Plk1 protein analysis, a piece of tumor tissues was lysed in 100 μL tissue lysis buffer (50 mM HEPES, pH 7.5, 150 mM NaCl, 1 mM EGTA, 2.5 mM EDTA, 10% glycerol, 0.1% Tween 20, 1 mM dithiothreitol, 10 mM glycerol 2-phosphate, 1 mM NaF, and 0.1 mM Na_3VO_4) freshly supplemented with Roche's Complete Protease Inhibitor Cocktail Tablets. The lysates were incubated on ice for a total of 30 min and vortexed every 5 min. The lysates were centrifuged for 10 min at 12 000*g*. Proteins were then detected by Western blot analyses as described above.

Immunohistochemical Analysis. Mice were sacrificed, and tumor tissues were excised 24 h after the last treatment. The tissues were fixed in 4% formaldehyde and embedded in paraffin for analysis. Paraffin-embedded 5 μm tumor sections were prepared for immunohistochemical analysis.

The proliferation of tumor cells was detected using an antibody against PCNA. Deparaffinized slides were boiled for 5 min in 0.01 M sodium citrate buffer (pH 6.0) in a pressure cooker for antigen retrieval. Subsequently, slides were allowed to cool for another 5 min in the same buffer. After several rinses in PBS and pretreatment with blocking medium for 5 min, slides were incubated with the PCNA antibody (Maxim Biotech., Fuzhou, China) diluted to 1:300 in antibody diluent solution for 20 min at room temperature and then at 4 °C overnight. After washing slides in Tris-buffered saline, a streptavidin–biotin system was used according to the manufacturer's instructions (BioGenex, San Ramon, CA). The slides were counterstained using Aquatex (Merck, Gernsheim, Germany).

The apoptosis of tumor cells following treatments was determined using the TUNEL method according to the manufacturer's instructions (Roche, Basel, Switzerland). All sections were examined under a Nikon TE2000 microscope (Tokyo Prefecture, Japan).

Statistical Analysis. The statistical significance of treatment outcomes was assessed using Student's *t* test; $p < 0.05$ was considered statistically significant in all analyses (95% confidence level).

Conflict of Interest: The authors declare no competing financial interest.

Acknowledgment. This work was supported by the National Natural Science Foundation of China (51125012), the National Basic Research Program of China (973 Programs, 2010CB934001 and 2009CB930301), the Specialized Research Fund for the Doctoral Program of Higher Education from the Ministry of Education of China (SRFDP 20113402130008), the Fundamental Research Funds for the Central Universities (WK2070000008), and the Open Project of State Key Laboratory of Supramolecular Structure and Materials (SKLSSM201201).

Supporting Information Available: Additional figure of size distribution of the formed particles. This material is available free of charge *via* the Internet at http://pubs.acs.org.

REFERENCES AND NOTES

1. Davis, M. E.; Zuckerman, J. E.; Choi, C. H. J.; Seligson, D.; Tolcher, A.; Alabi, C. A.; Yen, Y.; Heidel, J. D.; Ribas, A. Evidence of RNAi in Humans from Systemically Administered siRNA *via* Targeted Nanoparticles. *Nature* **2010**, *464*, 1067–1070.
2. Kumar, P.; Ban, H. S.; Kim, S. S.; Wu, H. Q.; Pearson, T.; Greiner, D. L.; Laouar, A.; Yao, J. H.; Haridas, V.; Habiro, K.; *et al.* T Cell-Specific siRNA Delivery Suppresses HIV-1 Infection in Humanized Mice. *Cell* **2008**, *134*, 577–586.
3. Peer, D.; Park, E. J.; Morishita, Y.; Carman, C. V.; Shimaoka, M. Systemic Leukocyte-Directed siRNA Delivery Revealing Cyclin D1 as an Anti-inflammatory Target. *Science* **2008**, *319*, 627–630.
4. Alvarez-Erviti, L.; Seow, Y.; Yin, H.; Betts, C.; Lakhal, S.; Wood, M. J. A. Delivery of siRNA to the Mouse Brain by Systemic Injection of Targeted Exosomes. *Nat. Biotechnol.* **2011**, *29*, 341–345.
5. Bhirde, A. A.; Patel, V.; Gavard, J.; Zhang, G.; Sousa, A. A.; Masedunskas, A.; Leapman, R. D.; Weigert, R.; Gutkind, J. S.; Rusling, J. F. Targeted Killing of Cancer Cells *in Vivo* and *in Vitro* with EGF-Directed Carbon Nanotube-Based Drug Delivery. *ACS Nano* **2009**, *3*, 307–316.
6. Pecot, C. V.; Calin, G. A.; Coleman, R. L.; Lopez-Berestein, G.; Sood, A. K. RNA Interference in the Clinic: Challenges and Future Directions. *Nat. Rev. Cancer* **2011**, *11*, 59–67.
7. Whitehead, K. A.; Langer, R.; Anderson, D. G. Knocking Down Barriers: Advances in siRNA Delivery. *Nat. Rev. Drug Discovery* **2009**, *8*, 129–138.
8. Song, E. W.; Zhu, P. C.; Lee, S. K.; Chowdhury, D.; Kussman, S.; Dykxhoorn, D. M.; Feng, Y.; Palliser, D.; Weiner, D. B.; Shankar, P.; *et al.* Antibody Mediated *In Vivo* Delivery of Small Interfering RNAs *via* Cell-Surface Receptors. *Nat. Biotechnol.* **2005**, *23*, 709–717.

9. Hu-Lieskovan, S.; Heidel, J. D.; Bartlett, D. W.; Davis, M. E.; Triche, T. J. Sequence-Specific Knockdown of EWS-FLI1 by Targeted, Nonviral Delivery of Small Interfering RNA Inhibits Tumor Growth in a Murine Model of Metastatic Ewing's Sarcoma. *Cancer Res.* **2005**, *65*, 8984–8992.
10. Wang, Y.; Gao, S.; Ye, W.-H.; Yoon, H. S.; Yang, Y. Y. Co-delivery of Drugs and DNA from Cationic Core–Shell Nanoparticles Self-Assembled from a Biodegradable Copolymer. *Nat. Mater.* **2006**, *5*, 791–796.
11. Xiong, X. B.; Lavasanifar, A. Traceable Multifunctional Micellar Nanocarriers for Cancer-Targeted Co-delivery of MDR-1 siRNA and Doxorubicin. *ACS Nano* **2011**, *5*, 5202–5213.
12. Dassie, J. P.; Liu, X. Y.; Thomas, G. S.; Whitaker, R. M.; Thiel, K. W.; Stockdale, K. R.; Meyerholz, D. K.; McCaffrey, A. P.; McNamara, J. O., II.; Giangrande, P. H. Systemic Administration of Optimized Aptamer-siRNA Chimeras Promotes Regression of PSMA-Expressing Tumors. *Nat. Biotechnol.* **2009**, *27*, 839–846.
13. Semple, S. C.; Akinc, A.; Chen, J.; Sandhu, A. P.; Mui, B. L.; Cho, C. K.; Sah, D. W. Y.; Stebbing, D.; Crosley, E. J.; Yaworski, E.; *et al.* Rational Design of Cationic Lipids for siRNA Delivery. *Nat. Biotechnol.* **2010**, *28*, 172–176.
14. Zhou, J. B.; Patel, T. R.; Fu, M.; Bertram, J. P.; Saltzman, W. M. Octa-Functional PLGA Nanoparticles for Targeted and Efficient siRNA Delivery to Tumors. *Biomaterials* **2012**, *33*, 583–591.
15. Tseng, Y. C.; Mozumdar, S.; Huang, L. Lipid-Based Systemic Delivery of siRNA. *Adv. Drug Delivery Rev.* **2009**, *61*, 721–731.
16. Lv, H. T.; Zhang, S. B.; Wang, B.; Cui, S. H.; Yan, J. Toxicity of Cationic Lipids and Cationic Polymers in Gene Delivery. *J. Controlled Release* **2006**, *114*, 100–109.
17. Ma, Z.; Li, J.; He, F. T.; Wilson, A.; Pitt, B.; Li, S. Cationic Lipids Enhance siRNA-Mediated Interferon Response in Mice. *Biochem. Biophys. Res. Commun.* **2005**, *330*, 755–759.
18. Buyens, K.; Smedt, S. C. D.; Braeckmans, K.; Demeester, J.; Peeters, L.; Grunsven, L. A. V.; Jeu, X. D. M. D.; Sawant, R.; Torchilin, V.; Farkasova, K.; *et al.* Liposome Based Systems for Systemic siRNA Delivery: Stability in Blood Sets the Requirements for Optimal Carrier Design. *J. Controlled Release* **2012**, *158*, 362–370.
19. Heidel, J. D.; Yu, Z.; Liu, J. Y.-C.; Rele, S. M.; Liang, Y.; Zeidan, R. K.; Kornbrust, D. J.; Davis, M. E. Administration in Non-human Primates of Escalating Intravenous Doses of Targeted Nanoparticles Containing Ribonucleotide Reductase Subunit M2 siRNA. *Proc. Natl. Acad. Sci. U.S.A.* **2007**, *104*, 5715–5721.
20. DeMiguel, I.; Imbertie, L.; Rieumajou, V.; Major, M.; Kravtzoff, R.; Betbeder, D. Proofs of the Structure of Lipid Coated Nanoparticles (SMBV (TM)) Used as Drug Carriers. *Pharm. Res.* **2000**, *17*, 817–824.
21. Wong, H. L.; Bendayan, R.; Rauth, A. M.; Wu, X. Y. Simultaneous Delivery of Doxorubicin and GG918 (Elacridar) by New Polymer–Lipid Hybrid Nanoparticles (PLN) for Enhanced Treatment of Multidrug-Resistant Breast Cancer. *J. Controlled Release* **2006**, *116*, 275–284.
22. Thevenot, J.; Troutier, A. L.; David, L.; Delair, T.; Ladaviere, C. Steric Stabilization of Lipid/Polymer Particle Assemblies by Poly(ethylene glycol)-Lipids. *Biomacromolecules* **2007**, *8*, 3651–3660.
23. Zhang, L.; Chan, J. M.; Gu, F. X.; Rhee, J. W.; Wang, A. Z.; Radovic-Moreno, A. F.; Alexis, F.; Langer, R.; Farokhzad, O. C. Self-Assembled Lipid–Polymer Hybrid Nanoparticles: A Robust Drug Delivery Platform. *ACS Nano* **2008**, *2*, 1696–1702.
24. Salvador-Morales, C.; Zhang, L.; Langer, R.; Farokhzad, O. C. Immunocompatibility Properties of Lipid–Polymer Hybrid Nanoparticles with Heterogeneous Surface Functional Groups. *Biomaterials* **2009**, *30*, 2231–2240.
25. Chan, J. M.; Zhang, L.; Yuet, K. P.; Liao, G.; Rhee, J. W.; Langer, R.; Farokhzad, O. C. PLGA-Lecithin-PEG Core–Shell Nanoparticles for Controlled Drug Delivery. *Biomaterials* **2009**, *30*, 1627–1634.
26. Okada, H. One- and Three-Month Release Injectable Microspheres of the LH-RH Superagonist Leuprorelin Acetate. *Adv. Drug Delivery Rev.* **1997**, *28*, 43–70.
27. Saito, N.; Okada, T.; Horiuchi, H.; Murakami, N.; Takahashi, J.; Nawata, M.; Ota, H.; Nozaki, K.; Takaoka, K. A Biodegradable Polymer as a Cytokine Delivery System for Inducing Bone Formation. *Nat. Biotechnol.* **2001**, *19*, 332–335.
28. Yang, X. Z.; Dou, S.; Sun, T. M.; Mao, C. Q.; Wang, H. X.; Wang, J. Systemic Delivery of siRNA with Cationic Lipid Assisted PEG-PLA Nanoparticles for Cancer Therapy. *J. Controlled Release* **2011**, *156*, 203–211.
29. Thu, M. S.; Bryant, L. H.; Coppola, T.; Jordan, E. K.; Budde, M. D.; Lewis, B. K.; Chaudhry, A.; Ren, J.; Varma, N. R. S.; Arbab, A. S; *et al.* Self-Assembling Nanocomplexes by Combining Ferumoxytol, Heparin and Protamine for Cell Tracking by Magnetic Resonance Imaging. *Nat. Med.* **2012**, *18*, 463–467.
30. Xia, T.; Kovochich, M.; Liong, M.; Meng, H.; Kabehie, S.; George, S.; Zink, J. I.; Nel, A. E. Polyethyleneimine Coating Enhances the Cellular Uptake of Mesoporous Silica Nanoparticles and Allows Safe Delivery of siRNA and DNA Constructs. *ACS Nano* **2009**, *3*, 3273–3286.
31. Nakamura, T.; Akita, H.; Yamada, Y.; Hatakeyama, H.; Harashima, H. A Multifunctional Envelope-Type Nanodevice for Use in Nanomedicine: Concept and Applications. *Acc. Chem. Res.* **2012**, 10.1021/ar200254s.
32. Judge, A. D.; Robbins, M.; Tavakoli, I.; Levi, J.; Hu, L.; Fronda, A.; Ambegia, E.; McClintock, K.; MacLachlan, I. Confirming the RNAi-Mediated Mechanism of Action of siRNA-Based Cancer Therapeutics in Mice. *J. Clin. Invest.* **2009**, *119*, 661–673.
33. Bu, Y.; Yang, Z.; Li, Q.; Song, F. Silencing of Polo-like Kinase (Plk) 1 *via* siRNA Causes Inhibition of Growth and Induction of Apoptosis in Human Esophageal Cancer Cells. *Oncology* **2008**, *74*, 198–206.
34. Liu, X. Q.; Erikson, R. L. Polo-like Kinase (Plk) 1 Depletion Induces Apoptosis in Cancer Cells. *Proc. Natl. Acad. Sci. U.S.A.* **2003**, *100*, 5789–5794.
35. Davis, M. E.; Chen, Z.; Shin, D. M. Nanoparticle Therapeutics: An Emerging Treatment Modality for Cancer. *Nat. Rev. Drug Discovery* **2008**, *7*, 771–782.
36. Yang, X. Z.; Sun, T. M.; Dou, S.; Wu, J.; Wang, Y. C.; Wang, J. Block Copolymer of Polyphosphoester and Poly(L-Lactic Acid) Modified Surface for Enhancing Osteoblast Adhesion, Proliferation, and Function. *Biomacromolecules* **2009**, *10*, 2213–2220.
37. Savarala, S.; Ahmed, S.; Ilies, M. A.; Wunder, S. L. Stabilization of Soft Lipid Colloids: Competing Effects of Nanoparticle Decoration and Supported Lipid Bilayer Formation. *ACS Nano* **2011**, *5*, 2619–2628.
38. Schacher, F.; Betthausen, E.; Walther, A.; Schmalz, H.; Pergushov, D. V.; Muller, A. H. Interpolyelectrolyte Complexes of Dynamic Multicompartment Micelles. *ACS Nano* **2009**, *3*, 2095–2102.